King Saud University

Journal of Saudi Chemical Society

www.ksu.edu.sa
www.sciencedirect.com

ORIGINAL ARTICLE

Inhibiting effects of 2-mercapto-1-methylimidazole on copper corrosion in 0.5 M sulfuric acid

O. Benali [a,*], **L. Larabi** [b], **Y. Harek** [b]

[a] *Département de Biologie, Faculté des Sciences et de la Technologie, Université de Saïda, 20000 Saïda, Algeria*
[b] *Département de Chimie, Faculté des Sciences, Université Abou Bakr Belkaïd, 13000 Tlemcen, Algeria*

Abstract   The inhibiting efficiency of 2-mercapto-1-methylimidazole (MMI) on copper corrosion in sulfuric acid was investigated at 30 °C. Its effectiveness was assessed through electrochemical impedance spectroscopy, potentiodynamic polarization and gravimetric measurements. The results of study reveal that the inhibition efficiency of MMI depends on its concentration and attains approximately 81% at 10^{-4} M. The inhibitor was adsorbed on the copper surface according the Langmuir adsorption isotherm model. The value of standard free energy of adsorption was calculated from this isotherm.

1. Introduction

In order to reduce the corrosion of copper during surface treatments such as descaling and cleaning in acid pickling solutions, corrosion inhibitors are typically added. These include, for instances, imidazole derivatives, which are of interest of corrosion inhibitors for copper and its alloys (Chadwick and Hashemi, 1979; Yoshida and Ishida, 1985, 1995; Jang and

* Corresponding author.
E-mail address: benaliomar@hotmail.com (O. Benali).

Production and hosting by Elsevier

Ishida, 1992). On the other hand, it is known that benzotriazole (BTA) and its derivatives are excellent corrosion inhibitors for copper and its alloys in a wide range of media (Ling et al., 1995; Modestov et al., 1994; da Costa et al., 1990; Tommesani et al., 1997; Villamil et al., 2002) but the disadvantage of BTA is its toxicity. However, several investigators have studied the inhibitory effects of non-toxic compounds (Moretti et al., 2004; Fallavena et al., 2006; Bouyanzer et al., 2006; Raja and Sethuraman, 2008; Rahim et al., 2008; Chauhan and Gunasekaran, 2007; Abdel-Gaber et al., 2006). Moreover, Gašparac and Stupnišek-Lisac (1999) and Gašparac et al. (2000a,b) and Stupnišek-Lisac et al. (1998, 2000, 2002) studied the influence of imidazole derivatives which are compound with low toxicity. Our previous investigation has shown that 2-mercapto-1-methylimidazole (MMI) is good inhibitor for copper in 1 M HCl (Curkovic, 2009). This paper focuses on the efficiency of the same compounds as copper corrosion inhibitor in 0.5 M sulfuric acid. The MMI shows three anchoring sites suitable for surface bonding: the nitrogen atom, the sulfur atom and the aromatic ring.

The effect of the concentration of MMI on the corrosion of copper in sulfuric acid was studied using electrochemical and gravimetric methods. Its adsorption behavior was also investigated to determine the appropriate adsorption isotherm.

2. Experimental

2.1. Materials

The copper working electrode was of 99.94 purity. 2-Mercapto-1-methylimidazole (Merck) was used as received. Fig. 1 shows the molecular structures of MMI (two tautomers). The acid solutions were made from AR grade H_2SO_4 (Prolabo). Appropriate concentration of acid was prepared by using double-distilled water.

2.2. Electrochemical measurements

Disc electrode (0.5 cm^2 area) was prepared from the investigated copper. The electrode was polished with emery papers (from 400 to 1000), rinsed with distilled water, degreased by acetone, washed thoroughly with bi-distilled water and dried at room temperature. The concentration range of inhibitor employed was 5×10^{-5} to 10^{-4} M. The studies were carried out potentiodynamically in a thermostated electrolytic cell. Platinum disc was used as a counter-electrode (CE) and a saturated calomel electrode as a reference electrode (SCE). The latter was connected through a Luggin's capillary to the cell. The working electrode (WE) was immersed in a test solution for 2 h until a steady state open-circuit potential (E_{ocp}) was obtained. All experiments were conducted at 303 K.

The polarization curves and Nyquist diagrams were carried out in the absence and in the presence of various inhibitor concentrations with a PGZ301 potentiostat–galvanostat (VoltaLab40-Radiometer).The potentiodynamic current–potential curves were performed with scan rate 0.167 mV s^{-1}. The scan was first started from the E_{corr} until a potential $E = (E_{corr} -$ about 150 mV) and then from E_{corr} until a potential $E = (E_{corr} +$ about 150 mV). All the i_{corr} values were determined by extrapolation to E_{corr} of the anodic Tafel part. EIS measurements were carried out in frequency range from 10 kHz to 10 mHz with an amplitude of 10 mV peak-to-peak using a c signals at open-circuit potential. EIS spectra were analyzed by Zview impedance analysis software (Scribner Associates, Inc., Southern Pines, NC).

To test the reliability and reproducibility of the measurements, duplicate experiments were performed in each case of the same conditions.
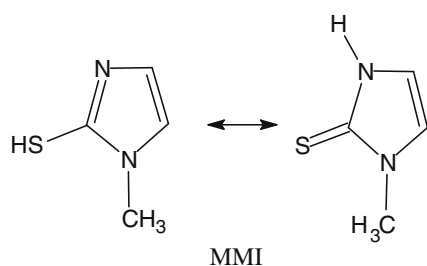
2.3. Gravimetric measurements

The specimens for weight loss measurements were 20 mm by 10 mm by 1 mm. They were polished with emery paper (from 400 to 1000 grade). Each run was carried out in a glass vessel containing 50 ml test solution. A clean weighed mild steel specimen was completely immersed at an inclined position in the vessel. After 2 h of immersion in H_2SO_4 0.5 M with and without addition of MMI at different concentrations, the specimen was withdrawn, rinsed with distilled water, washed with acetone, dried and weighed using an analytical balance accurate to 0.01 mg. The weight loss was used to calculate the corrosion rate in milligrams per square centimeter per hour.

3. Results and discussion

Polarization curves for copper electrode in 0.5 M H_2SO_4 in the absence and the presence of various concentrations of MMI are shown in Fig. 2. Values of associated electrochemical parameters and inhibitor efficiencies ($P\%$) of the studied compound are given in Table 1. The inhibitor efficiencies are defined as:

$$P\% = \frac{i_{corr}^0 - i_{corr}}{i_{corr}^0} \times 100, \tag{1}$$

where i_{corr}^0 and i_{corr} are the uninhibited and inhibited corrosion current densities, respectively.

Results given in Table 1 show that 10^{-4} M is an optimal concentration of MMI for copper corrosion protection in sulfuric acid. The corrosion potential E_{corr} shifted towards more cathodic values in the presence of MMI. This could be due to the fact that MMI had a strong effect on the oxygen reduction than the copper dissolution. The maximum of inhibition percentage ($P\%$) obtained was about 79% (10^{-4} M at 30 °C – 2 h).

From the Table 1, the slops of the cathodic Tafel line (b_c) and anodic Tafel lines are observed to change by the addition of the inhibitor compound, which indicates the influence of the MMI on the cathodic and anodic reactions, but the cathodic curves are more affected. The anodic slope values (b_a) rose with MMI concentration for more concentrated solutions and the cathodic slop values b_c decreases with MMI concentra-
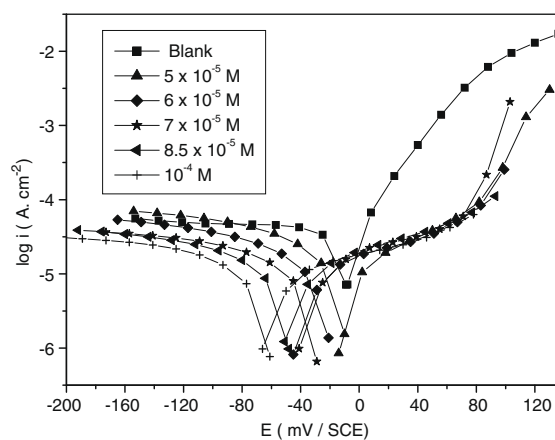

Figure 1 Molecular structures of MMI.

Figure 2 Potentiodynamic polarization curves for copper in 0.5 M H_2SO_4 containing different concentrations of MMI.

Table 1 Electrochemical parameters and the corresponding corrosion inhibition efficiencies for the corrosion of copper in 0.5 M H_2SO_4 containing different concentrations of MMI at 303 K.

Concentration (M)	b_c (mV/dec)	b_a (mV/dec)	$-E_{corr}$ (mV/SCE)	i_{corr} ($\mu A\ cm^{-2}$)	P (%)
Blank	1992	41.67	8	38	–
5×10^{-5}	236	125	10	11.75	69.08
6×10^{-5}	193	200	30	10.70	71.84
7×10^{-5}	283	162	36	10.25	73.03
8.5×10^{-5}	200	139	50	8.50	77.63
1×10^{-4}	222	188	65	8.20	78.42

tion. The Tafel anodic and cathodic slopes obtained in uninhibited 0.5 M sulfuric acid solution agreed with those reported in literature (Moretti et al., 2004; Stupnišek-Lisac et al., 2000; Larabi et al., 2006; Moretti and Guidi, 2004).

According to Mattson and Bockris (1959), the anodic dissolution of copper in sulfuric acid medium follows the mechanism given below:

$$Cu \leftrightarrow Cu^+_{ads} + \acute{e} \qquad (Fast) \qquad (2)$$
$$Cu^+_{ads} \leftrightarrow Cu^{2+}_{sol} + \acute{e} \qquad (Slow). \qquad (3)$$

The slope variation in the inhibited solution indicated a change in the copper dissolution. Unlike the two-electron electrodissolution mechanism, copper in the presence of MMI could (as for other inhibitors (Wu and Nobe, 1981) electrooxidized primarily to Cu^+ and is able to form slightly soluble $[Cu(MMI)_n]^+_{ads}$ complexes as the main electrooxidation products in the presence of a clean surface (Moretti and Guidi, 2004; Saban et al., 1998).
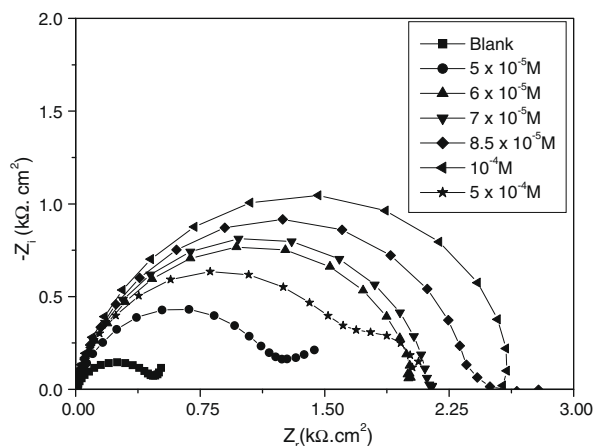
According to Smyrl (1981) the dissolution kinetic of copper in H_2SO_4 takes place through Eqs. (2) and (3). In the presence on inhibitor, this may participate, for example, in the intermediate formation $[Cu^+_{ads}]$, depending on the chemical stability and oxidative property of the adsorbed $[Cu(MMI)_n]^+_{ads}$ complex:

$$Cu^+_{ads} + nMMI \leftrightarrow [Cu(MMI)_n]^+_{ads}. \qquad (4)$$
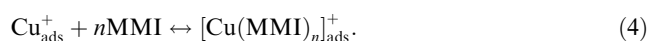
In the cathodic region, a little "hump" is observed at potentials close to E_{corr}, especially in the absence of inhibitor. This effect in interpreted as an additional cathodic process resulting from copper in deposition. This "hump" is not observed in the presence of inhibitor. This indicated a different mechanism of copper dissolution involving the participation of MMI.

Fig. 3 presents the electrochemical impedance spectroscopy diagrams at corrosion potential using the copper electrode in 0.5 M H_2SO_4, in the absence and presence of MMI at different concentrations. The impedance spectra measured in the case of absence of MMI and low concentrations of MMI, exhibited a Warburg impedance, indicating that the corrosion process involved the transport of reactants from the bulk solution to the copper/solution interface or transport of soluble corrosion products from the interface to the bulk solution in the early stage of corrosion. The Warburg impedance disappeared and the impedance spectra only displayed a depressed capacitive loop in the presence of MMI at 6×10^{-5} M. Moreover, the size of capacitive loop significantly increased with the further increase of the MMI concentration until 10^{-4} M. The changes of impedance spectra in size and shape with extension of the immersion time, including disappearance of the Warburg impedance and the increase of capacitive loop in size, show that a barrier gradually forms on the surface. The barrier is probably related to formation of the film of $[Cu(MMI)_n^+]$ complex. Note that for the concentrations of MMI higher than the optimal concentration the Nyquist spectra displayed two capacitive loops. The first capacitive loop, which is associated with the double layer relaxation, decreases. This result can be due to the degradation of the film.

Figure 3 Nyquist plots for copper in 0.5 M H_2SO_4 containing different concentrations of MMI.

Table 2 Impedance parameters and inhibition efficiency for the corrosion of copper in 0.5 M H_2SO_4 containing different concentrations of MMI at 303 K.

Concentration (M)	R_t ($\Omega\ cm^{-2}$)	Q ($\Omega^{-1}\ cm^{-2}\ s^n$)	n	C_{dl} ($\mu F\ cm^{-2}$)	P (%)
Blank	486	4×10^{-4}	0.70	198.25	–
5×10^{-5}	1413	1.4×10^{-4}	0.73	74.55	65.60
6×10^{-6}	2005	6.9×10^{-5}	0.84	48.18	75.76
7×10^{-5}	2105	6.6×10^{-5}	0.86	47.86	76.91
8.5×10^{-5}	2410	7.2×10^{-5}	0.87	55.42	79.83
1×10^{-4}	2548	5.95×10^{-5}	0.88	46.00	80.94

Impedance parameters derived from the Nyquist plots, percent inhibition efficiencies, P (%) and the equivalent circuit diagram are given in Table 2 and Fig. 4, respectively. The circuit consists of a constant phase element (CPE) Q, in parallel with a resistor R_t. The use of CPE-type impedance has been extensively described in Hukovic-Metikos et al. (2002), Mansfeld (1981) and McCafferty (1997).

$$Z_{CPE} \lfloor Q(jw)^n \rfloor^{-1}. \tag{5}$$

The above equation provides information about the degree of non-ideality in capacitance behavior. Its value makes it possible to differentiate between the behavior of an ideal capacitor ($n = 1$) and of a CPE ($n < 1$).

The percent inhibition efficiency is calculated by charge transfer resistance obtained from Nyquist plots, according to the equation:

$$P\% = \frac{R'_t - R_t}{R'_t} \times 100, \tag{6}$$

where R_t and R'_t are the charge transfer resistance values without and with inhibitor, respectively.

Considering that a CPE may be considered as a parallel combination of a pure capacitor and a resistor that is inversely proportional to the angular frequency, the value of capacitance, C_i, can thus be calculated for a parallel circuit composed of a CPE (Q) and a resistor (R_t), according to the following formula (Wu et al., 1999; Ma et al., 2003):

$$Q = \frac{(CR_t)^n}{R_t}. \tag{7}$$

The impedance spectra of copper in 0.5 M H_2SO_4 with and without inhibitor were analyzed by using the circuit in Fig. 4, and the double layer capacitance (C_{dl}) was calculated in terms of Eq. (7). Values of elements of the circuit corresponding to different corrosion systems, including values of C_{dl}, are listed in Table 2. As can be seen from this table the increase in resistance in the presence of MMI (compared to H_2SO_4 alone) is related to the corrosion protection effect of the molecules. The value of C_{dl} decreases in the presence of these inhibitors, suggesting that the MMI molecules function by adsorption at the metal solution/interface. It is important to point out that
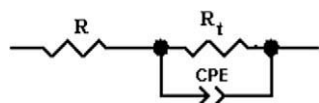
n increases in the presence of MMI reaching the value 0.88. This shows a decrease of the surface inhomogeneity as a result of the inhibitor's adsorption.

3.1. Weight loss measurements

Values of the inhibition efficiency and corrosion rate obtained from the weight loss measurements of copper for different concentrations of MMI in 0.5 M H_2SO_4 at 30 °C after 2 h of immersion are given in Table 3.

The inhibition efficiency is defined as follows:

$$P\% = \frac{W - W'}{W} \times 100, \tag{8}$$

where W and W' are the corrosion rates of copper due to the dissolution in 0.5 M H_2SO_4 in the absence and the presence of definite concentration of inhibitor, respectively.

MMI inhibits the corrosion of copper. It can be seen from Table 3 that inhibition efficiency increases with the increasing inhibitors concentration. Maximum $P\%$ of MMI was achieved at 8.5×10^{-5} M. These results are in reasonably good agreement with the values of inhibitor efficiency obtained from electrochemical techniques.

3.2. Adsorption isotherm

Basic information on the interaction between the inhibitor and the metal and the metal surface can be provided by the adsorption isotherm, which depends on the degree of electrode surface coverage θ. Data obtained from electrochemical impedance spectroscopy are used to analyze the adsorption mechanism, which θ is given by Zvauya and Dawson (1994):

$$\theta = \frac{R'_t - R_t}{R'_t}, \tag{9}$$

where R_t and R'_t are the charge transfer resistance values without and with inhibitor, respectively.

The surface coverage values (θ) were tested graphically to allow fitting of a suitable adsorption isotherm including Lamgmiu, Frumkin, Temkin, etc.

The plot of C/θ versus C for MMI is represented in Fig. 5. The data fit straight line, with slope nearly equal unity, indicat-

Figure 4 The equivalent circuit of the impedance spectra obtained for MMI.

Table 3 Corrosion rate of copper and inhibition efficiency for different concentrations of MMI for the corrosion of copper in 0.5 M H_2SO_4.

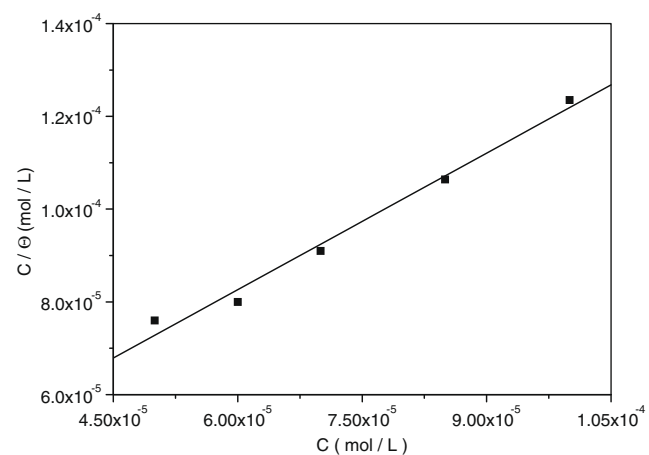| Concentration (M)	V_{corr} (mg cm^{-2} h^{-1})	P (%)
Blank	0.043	–
5×10^{-5}	0.017	60.46
6×10^{-6}	0.013	69.77
7×10^{-5}	0.012	72.09
8.5×10^{-5}	0.010	76.74
1×10^{-4}	0.010	76.74

Figure 5 Langmuir adsorption plot of copper in 0.5 M H_2SO_4 containing different concentrations of MMI.

ing that this compound adsorbs according to Langmuir adsorption isotherm where,

$$\theta = \frac{KC}{KC + 1}.$$ (10)

With

$$K = \left(\frac{1}{55.5}\right) \exp\left(-\frac{\Delta G_{ads}}{RT}\right),$$ (11)

where K is the equilibrium constant for the adsorption process, C is the concentration of the inhibitor.

The value of equilibrium adsorption constant obtained from this isotherm is about 4.21×10^4 L mol^{-1} suggesting a chemically adsorbed film (Villamil et al., 2002).

It is well known that values of $-\Delta G_{ads}$ of the order of 20 kJ mol^{-1} or lower indicate a physisorption mechanism; those of the order of 40 kJ mol^{-1} or higher involve charge sharing or a transfer from the inhibitor molecules to the metal surface to form a co-ordinate type of bond (Donahue and Nobe, 1965; Kamis et al., 1991).

The largest negative value of ΔG_{ads} (-36.94 kJ mol^{-1}) obtained here indicates that this inhibitor is strongly adsorbed onto the copper surface and is typical to chemisorption.

4. Conclusions

The main conclusions drawn from this study are:

– MMI inhibits the corrosion of copper in 0.5 M H$_2$SO$_4$.
– The inhibition is due to adsorption of the inhibitor molecules on the copper surface.
– The adsorption of MMI on the copper obeys the Langmuir adsorption isotherm model.
– Results obtained from dc polarization, ac impedance and weight loss techniques are in reasonably good agreement and show increased inhibitor efficiency with increasing inhibitor concentration.

References

Abdel-Gaber, A.M., Abd-El-Nabey, B.A., Sidahmed, I.M., El-Zayady, A.M., Saadawy, M., 2006. Corros. Sci. 48, 2765.
Bouyanzer, A., Hammouti, B., Majidi, L., 2006. Mater. Lett. 60, 2840.
Chadwick, D., Hashemi, T., 1979. Surf. Sci. 89, 649.
Chauhan, L.R., Gunasekaran, G., 2007. Corros. Sci. 49, 1143.
Curkovic, H.O., Stupnišek-Lisac, E., Takenouti, H., 2009. Corros. Sci. 51, 2342.

da Costa, S.F.L.A., Agostinlo, S.M.L., Rubim, J.C., 1990. J. Electroanal. Chem. 295, 203.
Donahue, F.M., Nobe, K., 1965. J. Electrochem. Soc. 112, 886.
Fallavena, T., Antonow, M., Gonçalves, R.S., 2006. Appl. Surf. Sci. 253, 566.
Gašparac, R., Stupnišek-Lisac, E., 1999. Corrosion 55, 1031.
Gašparac, R., Martin, C.R., Stupnišek-Lisac, E., 2000a. J. Electrochem. Soc. 147, 548.
Gašparac, R.R., Martin, C.R., Stupnišek-Lisac, E., Mandic, Z., 2000b. J. Electrochem. Soc. 147, 991.
Hukovic-Metikos, M., Babic, R., Grutac, Z., 2002. J. Appl. Electrochem. 32, 35.
Jang, J., Ishida, H., 1992. Corros. Sci. 33, 1053.
Kamis, E., Belluci, F., Latanision, R.M., El-Ashry, E.S.H., 1991. Corrosion 47, 677.
Larabi, L., Benali, O., Mekelleche, S.M., Harek, Y., 2006. Appl. Surf. Sci. 253, 1371.
Ling, Y., Guan, Y., Han, K.N., 1995. Corros. Sci. 51, 367.
Ma, H., Chen, S., Yin, B., Zhao, S., Liu, X., 2003. Corros. Sci. 45, 867.
Mansfeld, F., 1981. Corrosion 37, 301.
Mattson, E., Bockris, J.O'M., 1586. Trans. Faraday Soc. 55, 1586.
McCafferty, E., 1997. Corros. Sci. 39, 243.
Modestov, A.D., Zhou, G., Schwinsberg, D.P., 1994. Corros. Sci. 36, 1931.
Moretti, G., Guidi, F., 2004. Corros. Sci. 46, 387.
Moretti, G., Guidi, F., Grion, G., 2004. Corros. Sci. 46, 387.
Rahim, A.A., Rocca, E., Steinmetz, J., Kassim, M.J., 2008. Corros. Sci. 50, 1546.
Raja, P.B., Sethuraman, M.G., 2008. Mater. Lett. 62, 113.
Saban, A., Kalman, E., Telegedi, J., 1998. Electrochim. Acta 43, 159.
Smyrl, W.H., 1981. Copper dissolution kinetics in H$_2$SO$_4$. In: Bockris, O'M., Conway, B.E., Yeager, E., White, R.E. (Eds.). Comprehensive Treatise of Electrochemistry, vol. 4. Plenum Press, New York, p. 116.
Stupnišek-Lisac, E., Galic, N., Gašparac, R., 2000. Corrosion 56, 1105.
Stupnišek-Lisac, E., Loncaric Bozic, A., Cafuk, I., 1998. Corrosion 54, 713.
Stupnišek-Lisac, E., Gazivoda, A., Madzarac, M., 2002. Electrochim. Acta 47, 4189.
Tommesani, L., Brunoro, G., Frignani, A., Monticelli, C., Dal Colle, M., 1997. Corros. Sci. 39, 1221.
Villamil, R.F.V., Corio, P., Rubin, J.C., Agostinho, S.M.L., 2002. J. Electroanal. Chem. 535, 75.
Villamil, R.F.V., Cordeiro, G.G.O., Matos, J., D'Elia, E., Agostinho, S.M.L., 2002. Mater. Chem. Phys. 78, 448.
Wu, J.S., Nobe, K., 1981. Corrosion 37, 223.
Wu, X., Ma, H., Chen, S., Xu, Z., Sui, A., 1999. J. Electrochem. Soc. 146, 1847.
Yoshida, S., Ishida, H., 1985. Appl. Surf. Sci. 20, 497.
Yoshida, S., Ishida, H., 1995. Appl. Surf. Sci. 89, 39.
Zvauya, R., Dawson, J.L., 1994. J. Appl. Electrochem. 24, 943.